Mechanisms for the Deamination Reaction of Cytosine with H_2O/OH^- and $2H_2O/OH^-$: A Computational Study

Mansour H. Almatarneh, Christopher G. Flinn, and Raymond A. Poirier*

Department of Chemistry, Memorial University of Newfoundland, St. John's, Newfoundland, Canada A1B 3X7

Received August 29, 2007

Mechanisms for the deamination reaction of cytosine with H_2O/OH^- and $2H_2O/OH^-$ to produce uracil were investigated using ab initio calculations. Optimized geometries of reactants, transition states, intermediates, and products were determined at MP2 and B3LYP using the 6-31G(d) basis set and at B3LYP/6-31+G(d) levels of theory. Single point energies were also determined at MP2/G3MP2Large and G3MP2 levels of theory. Thermodynamic properties (ΔE, ΔH, and ΔG), activation energies, enthalpies, and free energies of activation were calculated for each reaction pathway investigated. Intrinsic reaction coordinate (IRC) analysis was performed to characterize the transition states on the potential energy surface. Seven pathways for the deamination reaction were found. All pathways produce an initial tetrahedral intermediate followed by several conformational changes. The final intermediate for all pathways dissociates to product via a 1−3 proton shift. The activation energy for the rate-determining step, the formation of the tetrahedral intermediate for pathway D, the only pathway that can lead to uracil, is 115.3 kJ mol^{-1} at the G3MP2 level of theory, in excellent agreement with the experimental value (117 ± 4 kJ mol^{-1}).

1. INTRODUCTION

A detailed knowledge of the structure of cytosine (Cyt) and its nucleoside as well as the tautomerism of nucleic acid bases is an important prerequisite in understanding the molecular basis underlying their biological and medicinal functions. The genetic code can be affected by tautomers of cytosine which can be recognized as other nucleic acid bases (i.e., uracil or thymine); in particular, rare tautomers are thought to induce alterations in the normal base pairing leading to spontaneous mutations and errors in the genetic code, in the DNA or RNA helices.[1] Cytosine occurs naturally in all nucleic acids, both DNA and RNA. It is chemically bound to the sugar moiety and interacts with other nucleic acid–bases via hydrogen bonds, most frequently with guanine.[2] For a more detailed review, see our previous work[3] and the references cited therein.

Mutations or changes to the nucleotide sequences of DNA can arise in a number of ways. Mistakes can be made during DNA replication that result in the incorporation of an incorrect base. Once altered, these changes may then be propagated by further DNA replication. Finally, large scale changes can sometimes occur in the form of DNA insertions and/or deletions. Spontaneous mutations can arise as a result of chemical changes to individual bases in DNA. One such chemical change is the conversion of cytosine to uracil (Ura) which is classified as a deamination reaction (the loss of an amino group from a tetrahedral carbon). The hydrolytic deamination reaction of cytosine to yield uracil is shown in Figure 1. Uracil is found in RNA and can base pair with adenine. It has firmly been established that deamination of the DNA base cytosine is an extremely rare event under normal physiological conditions (40–100 deamination in human genome per day, pH 7.4) although the rate of deamination can be significantly increased in the presence of various reagents such as NO, HNO_2 and bisulfite.

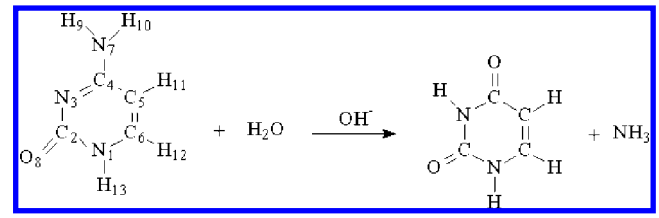

Figure 1. Deamination of cytosine with H_2O/OH^- and the atom labelling in cytosine.

If uracil is found in DNA, it poses a very serious problem. The cell, however, has a specific enzyme to remove it from DNA, called DNA uracil-*N*-glycosylase. The uracil formed by cytosine deamination is potentially mutagenic, changing the coding information during DNA replication and RNA transcription, resulting in altered base pairs in the genome.[4]

The deamination of cytosine, in particular, and a number of its derivatives have been the subject of many experimental studies.[5–15] Federico et al.[15] were able to determine the rate constant of cytosine deamination for single- and double-stranded DNA at physiological relevant conditions (37 °C and pH 7.4) by a sensitive genetic assay in which a mutant bacteriophage with a CCC codon is used with *E. coli* host cells defective in repair of uracil. Deamination to yield UCC or CUC lead to the generation of blue plaques, whereas, the CCC results in colorless plaques. Their measured rate constants for single- and double-stranded DNA are 1×10^{-10} and 7×10^{-13} s^{-1}, respectively, with an activation energy of 117 ± 4 kJ mol^{-1}. This value agrees well with the previous value of 121 kJ mol^{-1} found by Lindahl and

* Corresponding author. Tel.: (709) 737-8609. Fax: (709) 737-3702. E-mail: rpoirier@mun.ca.

10.1021/ci7003219 CCC: $40.75
Published on Web 04/02/2008

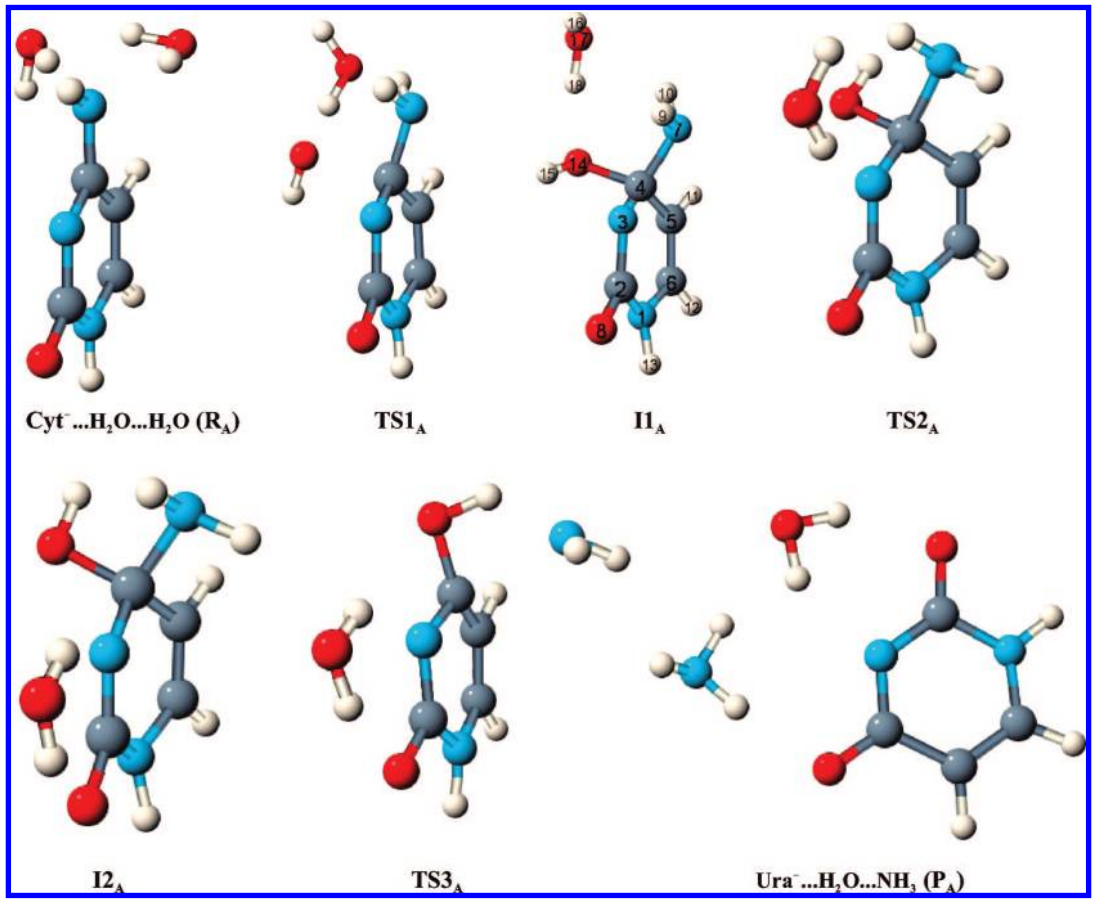

Figure 2. Optimized structures for the deamination of cytosine with H_2O/OH^- (pathway A).

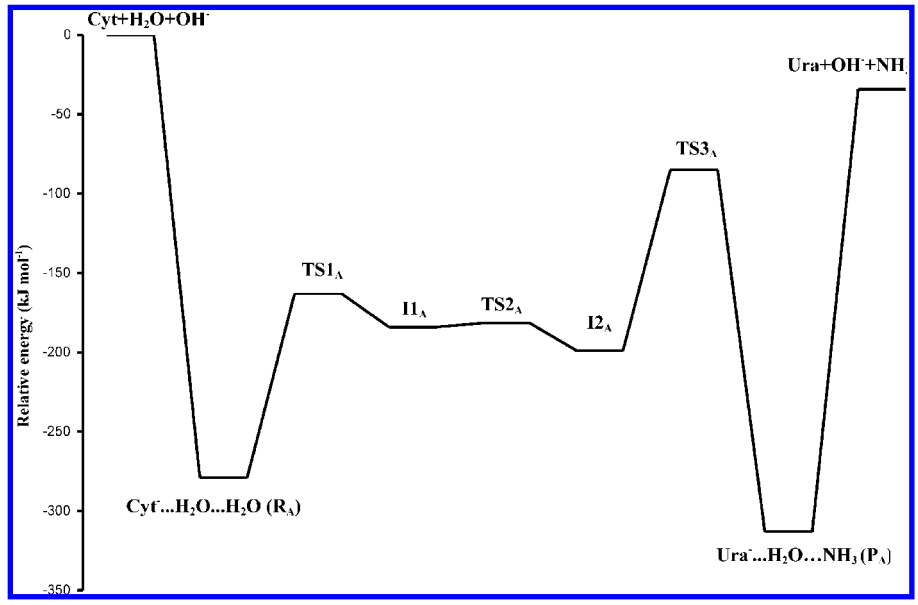

Figure 3. Reaction pathway A for the deamination of cytosine with H_2O/OH^-. Relative energies are at the G3MP2 level of theory.

Nyberg[16] obtained over a 25 °C temperature range. As a part of their investigation of the deamination of 1-methylcytosine and 1,5-dimethylcytosine with Pt^{II} complex, both experimentally and using DFT calculations, Sponer et al.[17] also studied the deamination of cytosine with OH^- using the PCM model to account for solvation effects. However, their reported activation energy barrier (213.4 kJ mol^{-1} at B3LYP/6-31G(d)) is not very close to the experimentally accepted value[15,16] (117 ± 4 kJ mol^{-1}), and the mechanism reported in their paper differs in a number of ways from the one reported in our previous work.[3] Rayat et al.[18] studied the nitrosative deamination of cytosine in DNA experimentally. They provided a mechanistic hypothesis for nitrosative cytosine deamination which involves a pyrimidine ring-opened intermediate and proposed a number of possible reaction channels. More recently, Matsubara et al.[19] studied the catalysis for cytidine deaminase. They also studied the uncatalysed hydrolytic deamination of cytosine with H_2O.

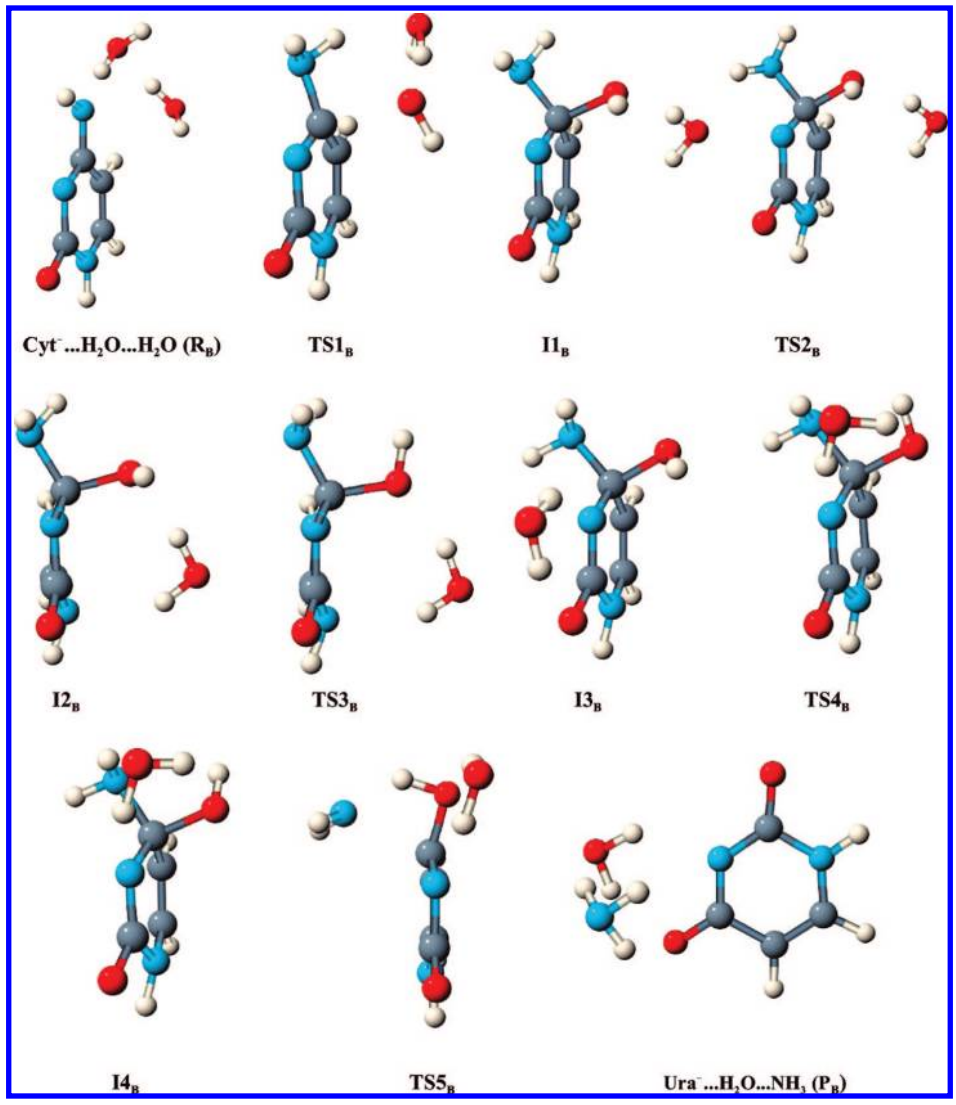

Figure 4. Optimized structures for the deamination of cytosine with H_2O/OH^- (pathway B).

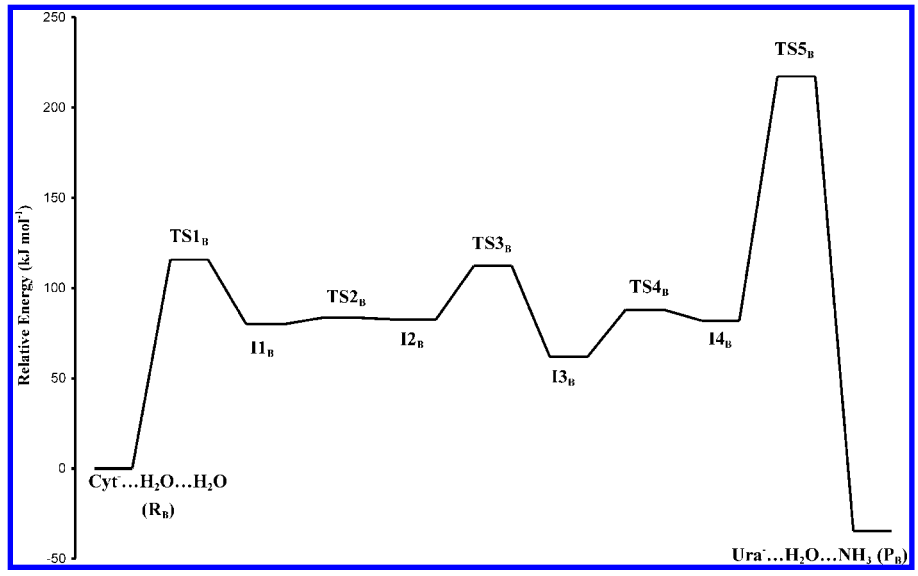

Figure 5. Reaction pathway B for the deamination of cytosine with H_2O/OH^-. Relative energies are at the G3MP2 level of theory.

They found that the catalytic action of cytidine deaminase is effectively enhanced by the participation of the extra water molecule. Their reported activation energy barrier with one water molecule is 237.4 kJ mol^{-1} at B3LYP/6-31G(d,p)). We have shown in previous work on the deamination of cytosine with H_2O, that this reaction is not the most likely

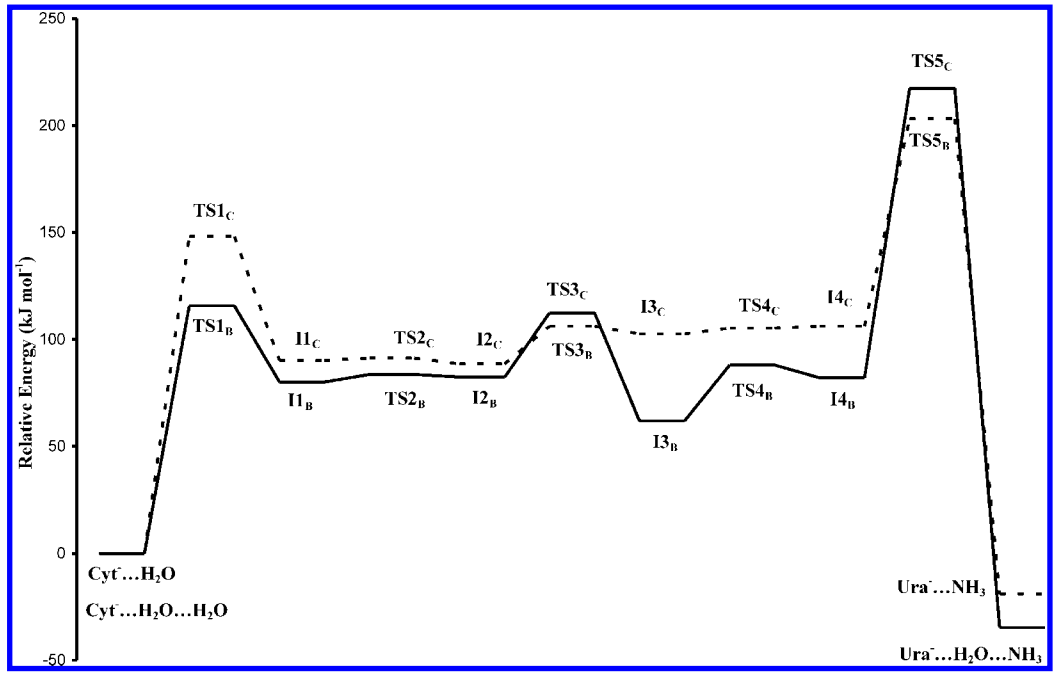

Figure 6. Comparison of reaction pathways for the deamination of cytosine with OH^- (dotted line)[3] and reaction pathway B for the deamination of cytosine with H_2O/OH^- at the G3MP2 level of theory.

Table 1. Activation Energies, Enthalpies of Activation, and Free Energies of Activation for the Deamination of Cytosine with H_2O/OH^- (in kJ mol^{-1}) at 298.15 K (Pathway A)

	MP2/ 6-31G(d)	B3LYP/ 6-31G(d)	B3LYP/ 6-31+G(d)	G3MP2
ΔE_{act}, $TS1_A$	137.1	130.7	118.4	115.3 (116.5)[a]
$\Delta H^{\ddagger}$, $TS1_A$	129.8	124.6	114.7	112.1
$\Delta G^{\ddagger}$, $TS1_A$	139.2	133.4	122.9	122.0
ΔE_{act}, $TS2_A$	8.2	7.5	4.6	2.5 (4.4)
$\Delta H^{\ddagger}$, $TS2_A$	5.6	4.4	2.4	0.9
$\Delta G^{\ddagger}$, $TS2_A$	5.1	4.6	7.7	2.5
ΔE_{act}, $TS3_A$	141.7	107.6	103.7	114.0 (125.8)
$\Delta H^{\ddagger}$, $TS3_A$	122.6	92.9	90.9	115.1
$\Delta G^{\ddagger}$, $TS3_A$	118.1	89.4	87.8	113.8

[a] The values in bracket are for MP2/G3MP2Large.

Table 2. Activation Energies, Enthalpies of Activation, and Free Energies of Activation for the Deamination of Cytosine with H_2O/OH^- (in kJ mol^{-1}) at 298.15 K (Pathway B)

	MP2/ 6-31G(d)	B3LYP/ 6-31G(d)	B3LYP/ 6-31+G(d)	G3MP2
ΔE_{act}, $TS1_B$	132.6	127.3	116.8	115.7 (120.2)[a]
$\Delta H^{\ddagger}$, $TS1_B$	129.3	122.7	114.0	113.3
$\Delta G^{\ddagger}$, $TS1_B$	144.4	135.8	123.3	122.4
ΔE_{act}, $TS2_B$	8.5	2.3	2.7	3.5 (4.2)
$\Delta H^{\ddagger}$, $TS2_B$	5.4	0.2	0.7	2.0
$\Delta G^{\ddagger}$, $TS2_B$	6.5	3.4	3.9	5.0
ΔE_{act}, $TS3_B$	45.4	41.4	35.1	29.9 (34.1)
$\Delta H^{\ddagger}$, $TS3_B$	41.2	36.8	30.4	29.0
$\Delta G^{\ddagger}$, $TS3_B$	42.1	37.5	30.8	29.9
ΔE_{act}, $TS4_B$	26.5	23.5	15.0	26.0 (26.3)
$\Delta H^{\ddagger}$, $TS4_B$	23.9	20.7	11.8	24.2
$\Delta G^{\ddagger}$, $TS4_B$	29.7	26.3	15.1	28.3
ΔE_{act}, $TS5_B$	144.7	112.2	100.7	115.2 (128.3)
$\Delta H^{\ddagger}$, $TS5_B$	124.6	95.9	88.1	113.5
$\Delta G^{\ddagger}$, $TS5_B$	115.3	88.5	84.7	70.5

[a] The values in bracket are for MP2/G3MP2Large.

mechanism to account for the deamination reaction of cytosine and hence not a model for similar systems, such as cytosine derivatives (Cytidine).[3]

Our previous results[3,20] were useful starting points for the proposed mechanisms in this paper. The deamination of cytosine with H_2O was found[3] to have a high activation energy (221.3 kJ mol^{-1} for pathway A and 260.3 kJ mol^{-1} for pathway B). The activation energy for the deamination reaction with OH^- was very high, with an overall activation energy of 203 kJ mol^{-1} at the G3MP2 level of theory, compared to the experimental value (117 ± 4 kJ mol^{-1}). This reaction takes place at physiological condition, pH 7.4, which is slightly basic. Federico et al.[15] suggested that the probability of deamination would increase by any process that would facilitate OH^- attack on the C_4 residue of cytosine. Since most proton transfers are mediated by water, one must consider the role of water molecules in the proton transfer. OH^- forms a strong hydrogen bond with H_2O and a stable complex. Computational studies have shown that interaction with water changes the relative energies of the cytosine tautomers, the canonical tautomer (the amino-oxo tautomer as shown in Figure 1) being better hydrated than the other tautomers.[21] The mechanism for the deamination of cytosine in DNA is unknown and the experimental activation energy was determined for cytosine deamination in single-stranded DNA. For these reasons, we have performed a detailed study of possible mechanisms for the deamination of cytosine with H_2O/OH^- and $2H_2O/OH^-$ in which the water molecules act as a solvent (and do not directly participate in the proton transfer process), as well as when they mediate the hydrogen transfer step.

2. COMPUTATIONAL METHOD

All the computations were performed with the Gaussian03 suite of programs.[22] The geometries of all reactants, transition states, intermediates, and products were fully optimized at MP2 and B3LYP levels of theory using the 6-31G(d) basis set and at B3LYP/6-31+G(d). Single point energies were determined at G3MP2 and the MP2/G3MP2Large levels of theory. We

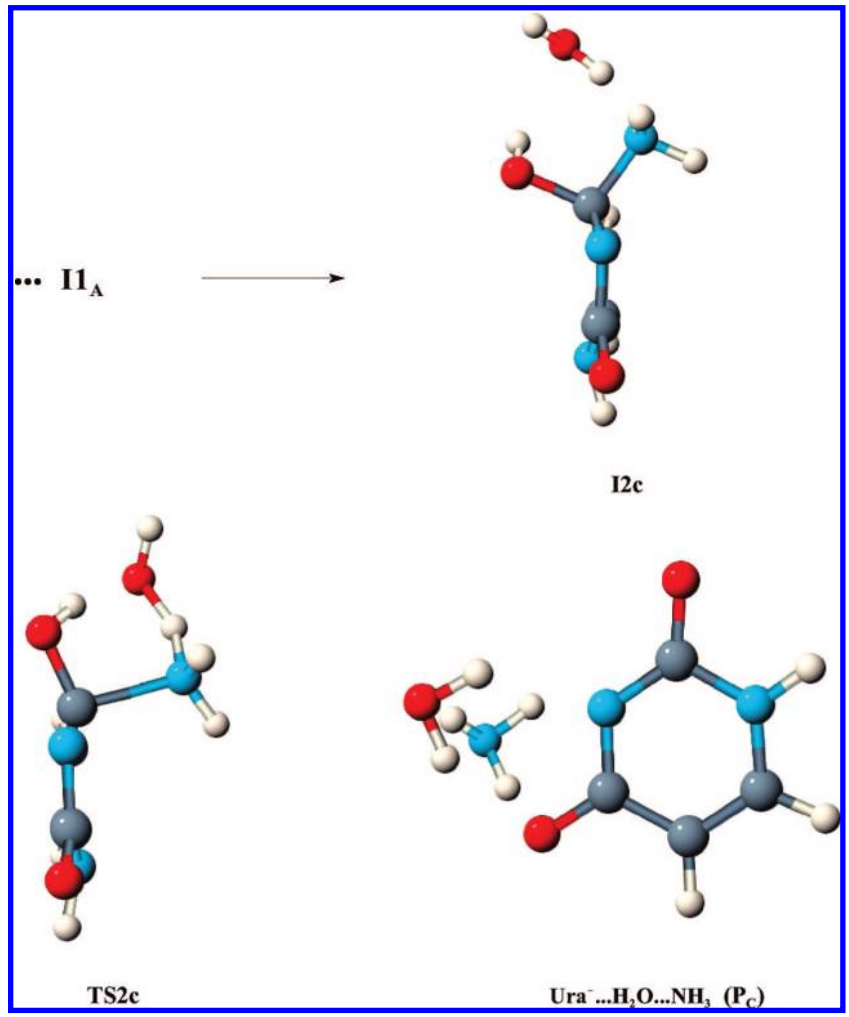

Figure 7. Optimized structures for the deamination of cytosine with H_2O/OH^- (pathway C).

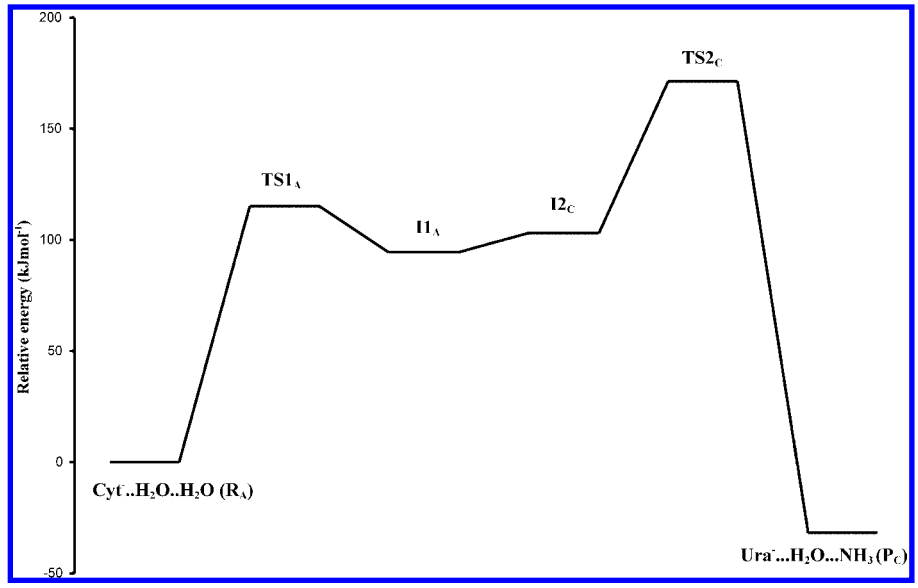

Figure 8. Reaction pathway C for the deamination of cytosine with H_2O/OH^-. Relative energies are at the G3MP2 level of theory.

chose the G3MP2 level of theory which is known to give reliable energetics as confirmed from our previous results.[23] The complete reaction pathway for each mechanism discussed in this paper has been verified using intrinsic reaction coordinate (IRC) analysis of all transition states. The structures at the last IRC points in both directions were further optimized, in order to positively identify the reactant and product to which each transition state is connected. A frequency analysis was performed for each stationary point in order to ensure that all minima had no imaginary frequencies on the potential-energy surface and that transition states have a single imaginary frequency.

Table 3. Activation Energies, Enthalpies of Activation, and Free Energies of Activation for the Deamination of Cytosine with H_2O/OH^- (in kJ mol^{-1}) at 298.15 K (Pathway C)

	MP2/ 6-31G(d)	B3LYP/ 6-31G(d)	B3LYP/ 6-31+G(d)	G3MP2
ΔE_{act}, $TS1_A$	137.1	130.7	118.4	115.3 (116.5)[a]
$\Delta H^{\ddagger}$, $TS1_A$	129.8	124.6	114.7	112.1
$\Delta G^{\ddagger}$, $TS1_A$	139.2	133.4	122.9	122.0
ΔE_{act}, $TS2_C$	73.0	52.2	50.2	68.3 (65.3)
$\Delta H^{\ddagger}$, $TS2_C$	59.7	36.6	41.4	65.2
$\Delta G^{\ddagger}$, $TS2_C$	66.3	42.1	51.7	68.3

[a] The values in bracket are for MP2/G3MP2Large.

3. RESULTS AND DISCUSSION

Cytosine has significant hydrogen bonding abilities; in particular, it possesses both hydrogen bond donor and acceptor groups. For this reason, we have examined a number of possible hydrogen-bonded complexes between H_2O, OH^-, and cytosine. We found that adding H_2O and OH^- to the $N_7-C_4-C_5-C_6$ side produced higher activation energies than adding them to the $N_7-C_4-N_3-C_2$ side of cytosine (see Figure 1). In addition, since it is the $N_7-C_4-N_3-C_2$ side of cytosine that hydrogen bonds with other nucleic acid–bases (normally guanine), it is more sterically hindered.[2] Adding one water molecule stabilized the transition states and destabilized the reactant complex $Cyt^-\cdots H_2O$. Deamination of cytosine with H_2O/OH^- and $2H_2O/OH^-$ can follow several possible pathways designated as pathways A → D and F → H.

3.1. Deamination of Cytosine with H_2O/OH^-: Pathways A and B. In our previous work, we found two energetically equivalent pathways for the deamination of cytosine with OH^- which involve OH^- attack on both faces of cytosine.[3] However, due to lack of symmetry, the extra water molecule now results in two different pathways (A and B) for attack on the two faces of cytosine.

Pathway A. The geometries for the reactants, intermediates, transition states, and products involved in pathway A (OH^- attack on the left face of cytosine with the carbonyl group facing the observer) are shown in Figure 2, and their relative energies are given in Figure 3.

For comparison, Figure 3 shows the relative stability of (Cyt + H_2O + OH^-) and the ($Cyt^-\cdots H_2O\cdots H_2O$) complex which is highly stabilized partly due to the delocalized negative charge on the cytosine anion compared to OH^-. Deamination of cytosine with H_2O/OH^- (Cyt + OH^- + H_2O → Ura + NH_3 + OH^-) closely follows the mechanism for the deamination of cytosine with H_2O and as well as the deamination with OH^-,

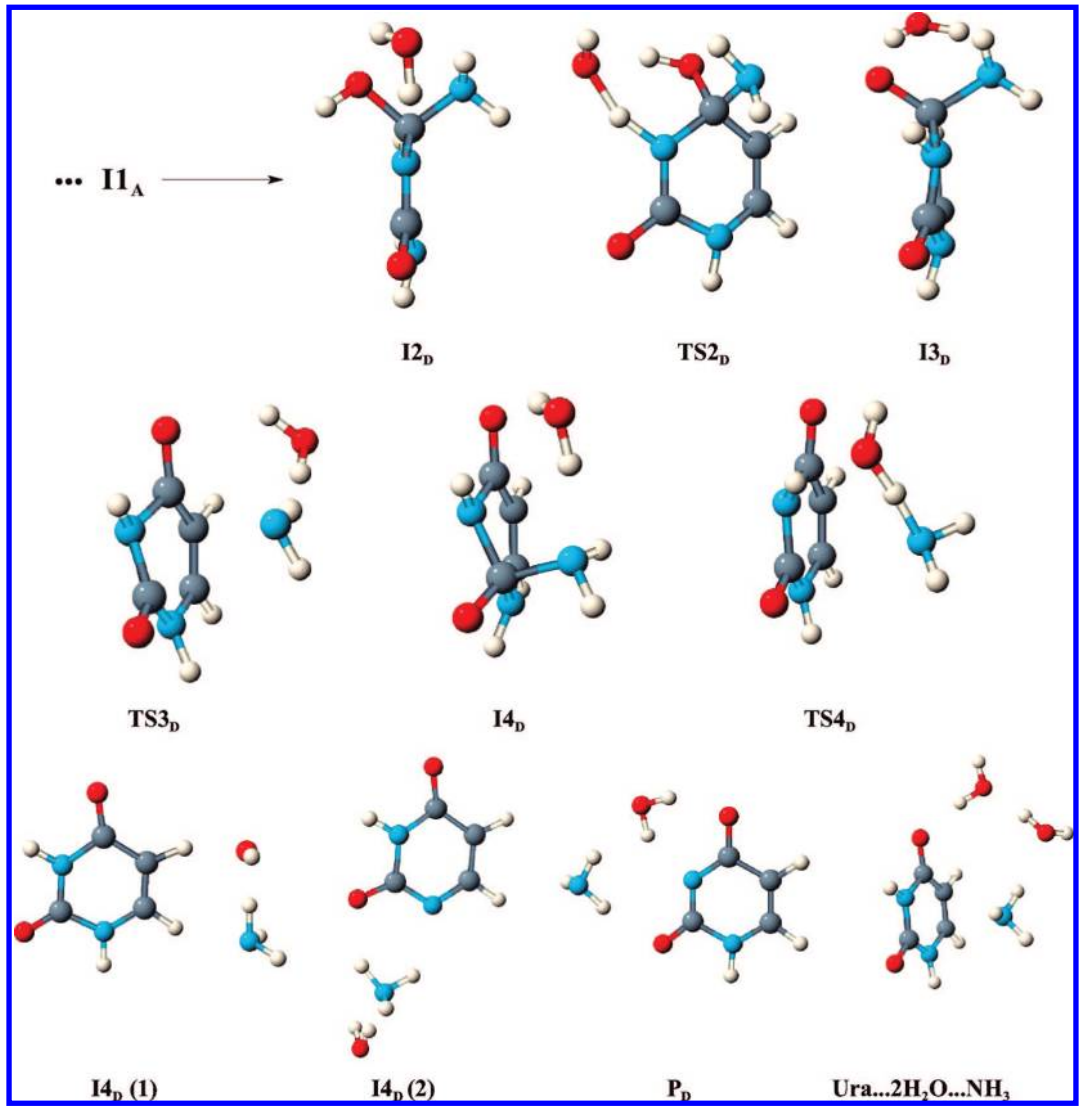

Figure 9. Optimized structures for the deamination of cytosine with H_2O/OH^- (pathway D).

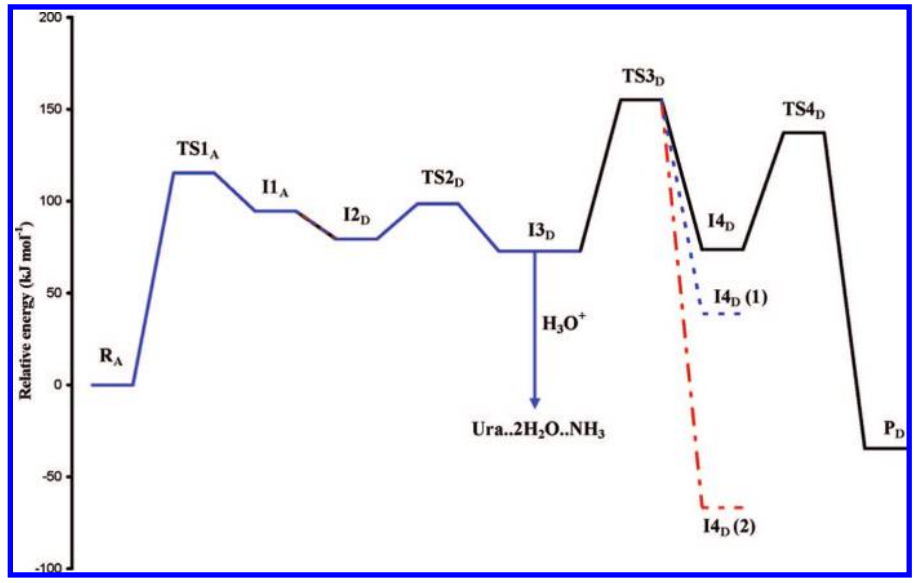

Figure 10. Reaction pathway D for the deamination of cytosine with H_2O/OH^-. Relative energies are at the G3MP2 level of theory. The $I4_D(1)$ optimized structure is at B3LYP/6-31G(d), and $I4_D(2)$ is at B3LYP/6-31+G(d) and HF/6-31G(d) (see the Supporting Information).

Table 4. Activation Energies, Enthalpies of Activation, and Free Energies of Activation for the Deamination of Cytosine with H_2O/OH^- (in kJ mol^{-1}) at 298.15 K (Pathway D)

	MP2/ 6-31G(d)	B3LYP/ 6-31G(d)	B3LYP/ 6-31+G(d)	G3MP2
ΔE_{act}, $TS1_A$	**137.1**	**130.7**	**118.4**	**115.3 (116.5)**[a]
$\Delta H^{\ddagger}$, $TS1_A$	129.8	124.6	114.7	112.1
$\Delta G^{\ddagger}$, $TS1_A$	139.2	133.4	122.9	122.0
ΔE_{act}, $TS2_D$	37.9	27.0	21.6	19.2 (25.3)
$\Delta H^{\ddagger}$, $TS2_D$	23.8	12.3	8.0	16.6
$\Delta G^{\ddagger}$, $TS2_D$	28.6	16.5	16.1	22.8
ΔE_{act}, $TS3_D$	120.9	95.2	69.4	82.4 (93.6)
$\Delta H^{\ddagger}$, $TS3_D$	108.3	76.7	58.0	83.9
$\Delta G^{\ddagger}$, $TS3_D$	107.3	68.4	59.4	81.5
ΔE_{act}, $TS4_D$	87.7	55.0	73.4[b]	63.6 (78.7)
$\Delta H^{\ddagger}$, $TS4_D$	73.4	47.0	51.6	64.4
$\Delta G^{\ddagger}$, $TS4_D$	78.8	59.4	58.0	62.3

[a] The values in bracket are for MP2/G3MP2Large. Bold numbers are indicating the rate-determining step for this pathway. [b] $TS4_D$ did not converge to a first-order saddle point at B3LYP/6-31+G(d) but converged to the product; the value reported is for B3LYP/6-31+G(d)//HF/6-31G(d).

particularly, in relation to the two rate-determining steps. The first rate-determining step involves formation of a tetrahedral intermediate ($I1_A$), followed by a conformational change and a second rate-determining step which is a 1–3 proton shift from the hydroxy group to the exocyclic nitrogen atom.

Pathway A has two rate-determining steps. Deprotonation of cytosine occurs easily without forming a Cyt$\cdots H_2O\cdots OH^-$ complex. The H_{10} immediately transfers to OH^- forming a water molecule and a more stable ($Cyt^-\cdots 2H_2O$) complex which is the reactant for pathways A, B, C, and D. In the first rate-determining step, the addition of a water molecule stabilizes the hydroxide ion being formed in the transition state ($TS1_A$), dropping the activation energy. Nucleophilic attack by the water molecule on the C_4 carbon atom occurs with simultaneous proton transfer from H_2O to the exocyclic imine nitrogen of the cytosine anion to form a tetrahedral intermediate ($I1_A$). This is followed by a conformational change to give a second intermediate $I2_A$ in which the water molecule has migrated to be in the same plane as the cytosine ring, with an activation energy of only 2.5 kJ mol^{-1} at G3MP2. Conformers $I1_A$ and $I2_A$ only differ with respect to the position of the water molecule, the torsion of H_{15} ($H_{15}O_{14}C_4N_3$), and the torsion of the hydrogen atoms (H_9 and H_{10}) which are connected to N_7. See the atom labeling for $I1_A$ in Figure 2. The conformational change is followed by an intramolecular 1–3 proton shift from the hydroxyl group to the amino group to yield a $Ura^-\cdots H_2O\cdots NH_3$ complex. This mechanism is similar to the deamination of cytosine with OH^-.[3] However, addition of a single water molecule stabilizes the transition states of both rate-determining steps lowering the overall activation energy by 8.9 kJ mol^{-1}.

Pathway B. The optimized structures involved in pathway B are shown in Figure 4, while the relative energies are given in Figure 5. Pathway B also has two rate-determining steps. As in pathway A, one of the H_2O attacks the C_4 carbon atom with simultaneous proton transfer to the imino group (sp^2 exocyclic nitrogen) of cytosine producing a tetrahedral intermediate, $I1_B$. This is followed by several low barrier conformational changes connecting intermediates $I1_B$ and $I4_B$. In our previous work on the deamination of cytosine with H_2O and OH^-, we obtained two intermediate conformers with H_2O and three with OH^-. These conformers are different due to the existence of the two functional groups ($-NH_2$ and $-OH$) and H_2O in this system resulting in extra degrees of freedom. These structures are very similar, differing mainly in the torsion and the angles of these functional groups. The activation energies for the conformational changes are very small as expected and do not have a significant effect on the mechanism of this reaction. The final step is a 1–3 proton shift from the hydroxy group to the exocyclic nitrogen of the tautomer ($I4_B$) which results in the uracil anion deamination product; see Figure 4.

Figure 6 shows a comparison of the reaction pathways for the deamination of cytosine with OH^- and with H_2O/OH^- for pathway B. It can be seen from Figure 6 that the addition of a water molecule results in a slightly higher overall barrier for deamination.

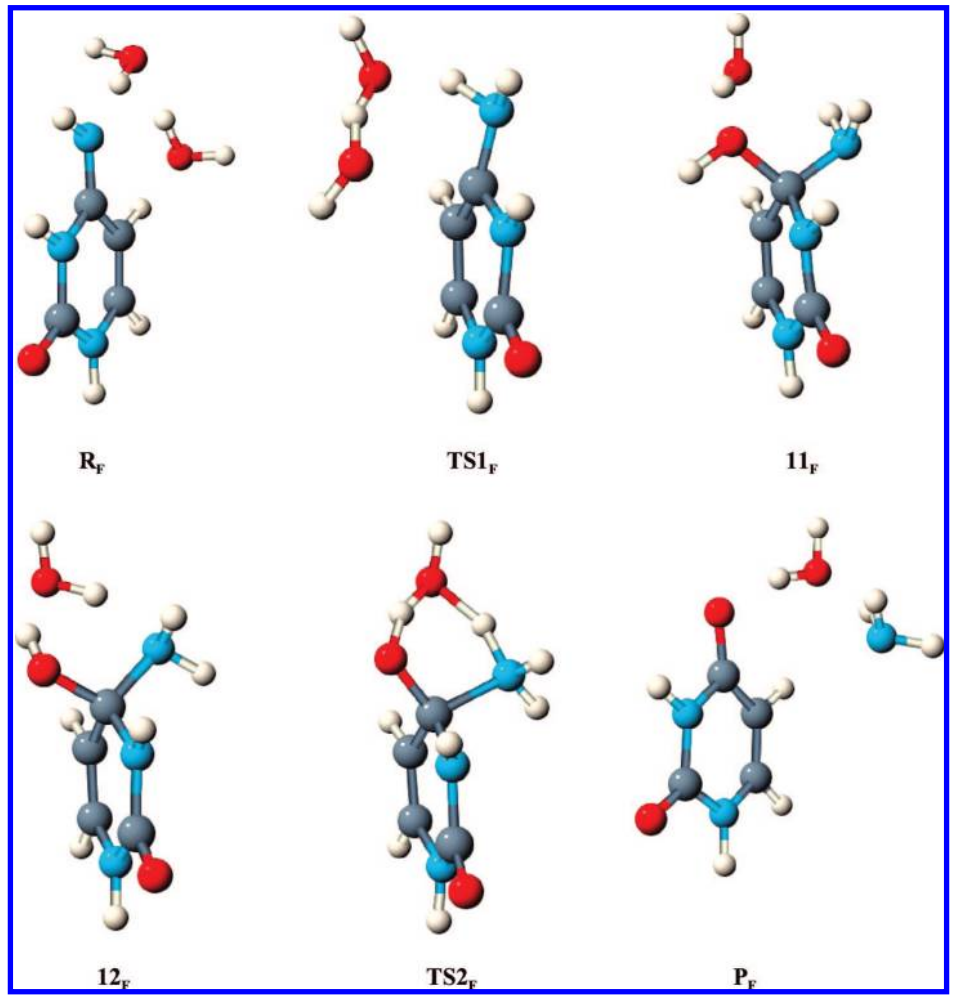

Figure 11. Optimized structures for the deamination of the amino-oxo tautomer of cytosine with $2H_2O$ (pathway F).

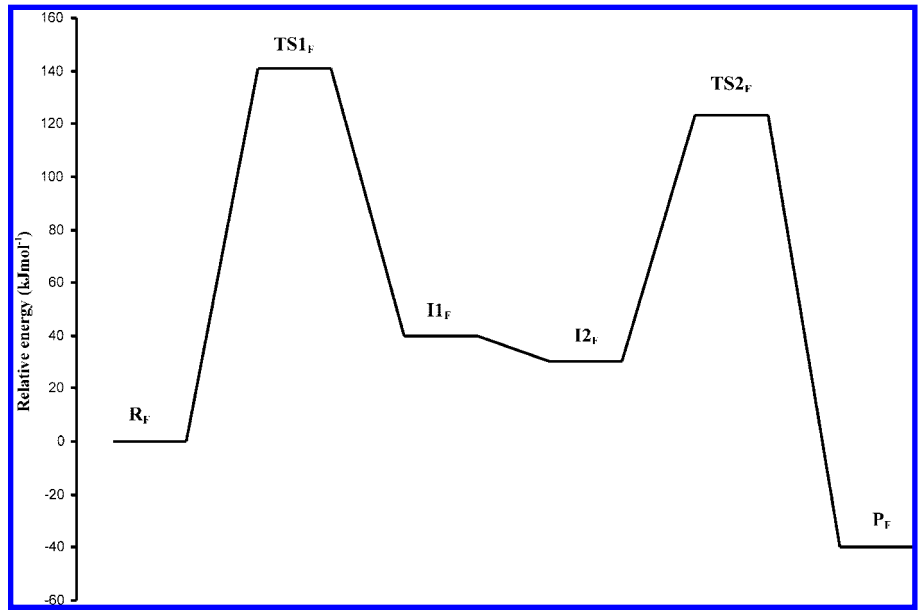

Figure 12. Reaction pathway F for the deamination of the amino-oxo tautomer of cytosine with $2H_2O$. Relative energies are at the G3MP2 level of theory.

The activation energies, enthalpies of activation, and free energies of activation for the deamination of cytosine with H_2O/OH^- at the MP2 and B3LYP levels of theory using the 6-31G(d) basis set, B3LYP/6-31+G(d), and G3MP2 levels of theory for both pathways A and B are listed in Tables 1 and 2, respectively. Activation energies of 117 ± 4 and 121 kJ mol^{-1} were reported experimentally for this reaction.[15,16] In our preliminary computational study,[3] the activation energies for the two rate-determining steps are 148.0 and 97.0 kJ mol^{-1} resulting in an overall activation energy of 203.1 kJ mol^{-1}; see Figure 6. In this study, the activation energies for the two rate-determining steps are 115.3 and 114.0

Table 5. Activation Energies, Enthalpies of Activation, and Free Energies of Activation for the Deamination of the Amino-oxo Tautomer of Cytosine with H_2O/OH^- (in kJ mol^{-1}) at 298.15 K (Pathway F)

	MP2/ 6-31G(d)	B3LYP/ 6-31G(d)	B3LYP/ 6-31+G(d)	G3MP2
ΔE_{act}, $TS1_F$	155.9	140.4	129.6	140.9 (141.8)[a]
$\Delta H^{\ddagger}$, $TS1_F$	140.9	125.0	116.3	135.1
$\Delta G^{\ddagger}$, $TS1_F$	159.4	140.1	129.5	153.8
ΔE_{act}, $TS2_F$	93.8	80.6	81.6	92.6 (91.1)
$\Delta H^{\ddagger}$, $TS2_F$	74.4	61.4	63.4	88.2
$\Delta G^{\ddagger}$, $TS2_F$	80.8	68.0	70.7	99.2

[a] The values in bracket are for MP2/G3MP2Large.

kJ mol^{-1} for pathway A and 115.7 and 115.2 kJ mol^{-1} for pathway B at the G3MP2 level of theory. Therefore, the overall activation energies for pathways A and B are 194.2 and 197.1 kJ mol^{-1} at G3MP2 and 192.7 and 193.7 kJ mol^{-1} at the B3LYP/6-31+G(d) level of theory, respectively. The MP2/G3MP2Large results for the barriers, are in excellent agreement with the G3MP2 values, differing by no more than 13 kJ mol^{-1} as shown in Tables 1 and 2. Furthermore, Tables 1 and 2 show that the computationally less expensive B3LYP/6-31+G(d) results are in good agreement with the G3MP2 differing by no more than 18 kJ mol^{-1} in this study.

3.2. Deamination of Cytosine with H_2O/OH^-: Pathways C and D. The overall activation energies for the deamination of cytosine with H_2O/OH^- for both pathways A and B are still high compared to the experimental value. In addition, the extra water molecule for pathways A and B did not participate in the 1–3 proton shift. It was previously reported that the formation of uracil (second step) from the tetrahedral intermediate is the rate-determining step.[6,24] For this step, we examined the role of the water molecule as a mediator on the 1−3 proton shift from the −OH group to the $-NH_2$ group which is one of the rate-determining steps of the catalytic process. It is well-known that water can act not only as a solvent but as a catalyst where it can donate or accept a proton to promote long-range proton transfer.[20,23] From our previous study on the decomposition reaction of

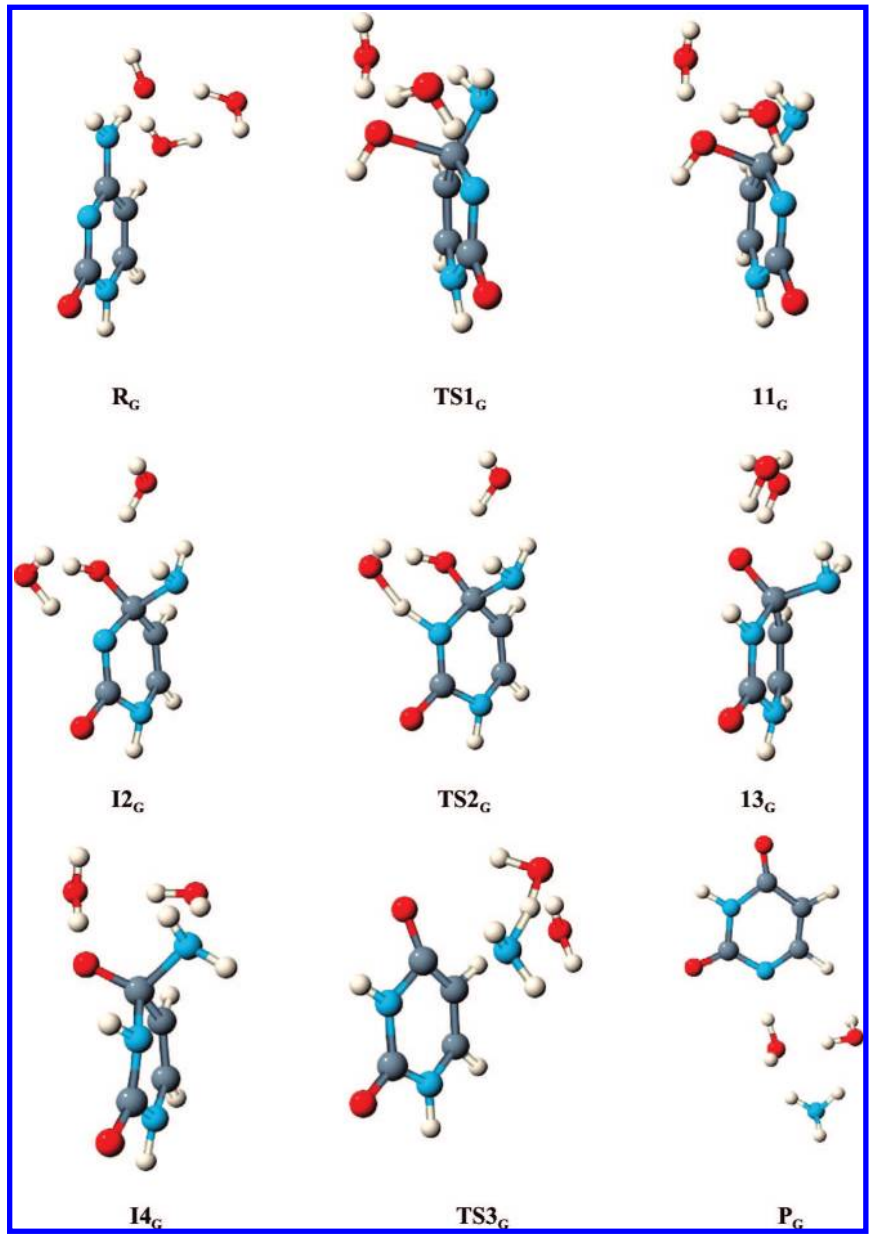

Figure 13. Optimized structures for the deamination of cytosine with $2H_2O/OH^-$ (pathway G).

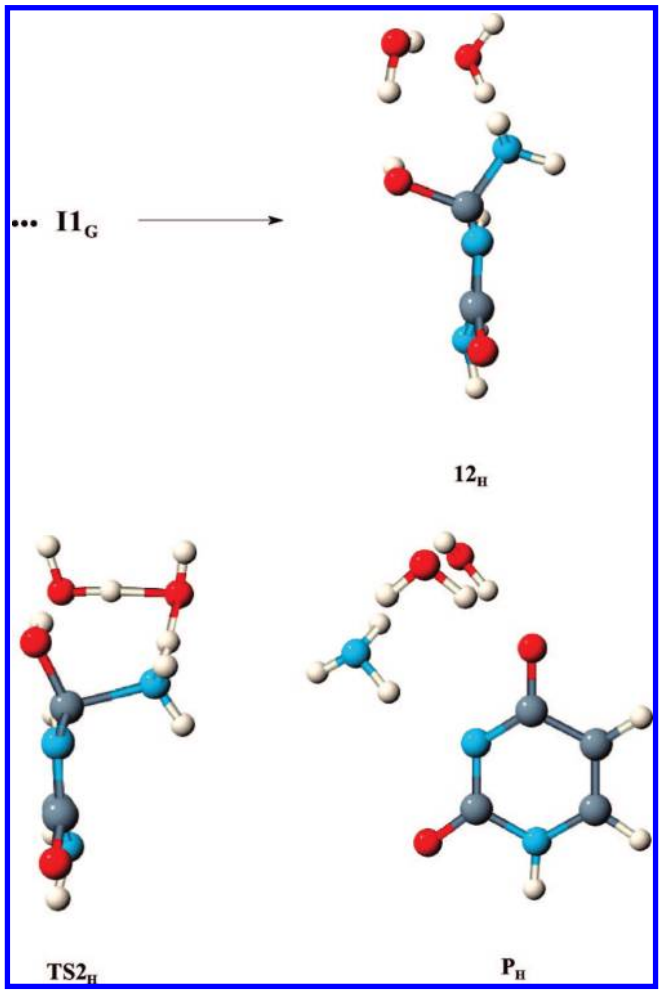

Figure 14. Optimized structures for the deamination of cytosine with $2H_2O/OH^-$ (pathway H).

formamidine,[23] we found that adding one water molecule catalyzed the 1–3 proton shift by forming a cyclic hydrogen-bonded transition state reducing the barrier by 88.4 kJ mol^{-1} at G3MP2. Addition of a second water molecule, further reduced the barrier by 17.2 kJ mol^{-1} at G3MP2.

Pathway C. The optimized structures and the relative energies involved in pathway C are shown in Figures 7 and 8, respectively. The activation energies, enthalpies of activation, and free energies of activation for the deamination of cytosine with H_2O/OH^- at MP2 and B3LYP levels of theory using the 6-31G(d) basis set, B3LYP/6-31+G(d), and G3MP2 levels of theory for pathway C are listed in Table 3. The first transition state for pathway C is the same as pathway A.

Intermediates $I1_A$ and $I2_C$ are connected with several conformational changes, which do not have a significant effect on the mechanism of this reaction and hence are not included in the figures. The barrier for the water-mediated 1–3 proton shift is reduced by 45.7 kJ mol^{-1} at G3MP2 and 53.5 kJ mol^{-1} at B3LYP/6-31+G(d) levels of theory. The activation energy for this step is 68.3 kJ mol^{-1} at G3MP2 and 50.2 kJ mol^{-1} at B3LYP/6-31+G(d). However, the overall activation energy is still somewhat high, 171.1 kJ mol^{-1} (160.6 kJ mol^{-1} at B3LYP/6-31+G(d)); see Table 3.

Pathway D. The optimized structures involved in pathway D are shown in Figure 9, and their relative energies given in Figure 10. The activation energies, enthalpies of activation, and free energies of activation for the deamination of cytosine with H_2O/OH^- at MP2 and B3LYP levels of theory using the 6-31G(d) basis set, B3LYP/6-31+G(d), and G3MP2 levels of theory for pathway D are listed in Table 4.

Of all the pathways investigated, pathway D (Figure 9) is the only pathway that can lead to neutral uracil for this system. The first step for pathway D is the same as pathway A. In this case, intermediate $I1_A$ is converted to $I2_D$ by conformational changes. Intermediate $I2_D$ undergoes a water-mediated 1−3 proton shift, from the −OH to the N_3 atom, to form intermediate $I3_D$ through $TS2_D$. The activation energy for $TS2_D$ is 19.2 kJ mol^{-1} at G3MP2; see Table 4. At the MP2/6-31G(d) level of theory, intermediate $I3_D$ is converted to intermediate $I4_D$ through transition state $TS3_D$, where the $-NH_2$ group is migrating from C_4 to C_2 (the carbonyl carbon), with the negative charge localized at O_8. In this case the IRC analysis resulted in two other possible intermediates, $I4_D(1)$ at B3LYP/6-31G(d) and $I4_D(2)$ at HF/6-31G(d) (see the Supporting Information) and B3LYP/6-31+G(d) levels of theory. From intermediate $I4_D$, a proton transfers from the oxygen of H_2O to the $-NH_2$ group with simultaneous transfer of a proton from the N_3 atom of uracil, through $TS4_D$, to form a $Ura^-\cdots H_2O\cdots NH_3$ complex (P_D) with the negative charge at N_3. For pathway D (R to P_D), the overall activation energy is 155.2 and 135.0 kJ mol^{-1} at G3MP2 and B3LYP/6-31+G(d) levels of theory, respectively.

However, in reality (in DNA or in solution), intermediate $I3_D$, as shown in Figure 9, would most likely be protonated at the $-NH_2$ group to form ammonia resulting in a complex of $Ura\cdots 2H_2O\cdots NH_3$. In this case, the first step is the rate-determining step with an activation energy of 115.3 and 118.4 kJ mol^{-1} at G3MP2 and B3LYP/6-31+G(d) levels of theory, respectively, which accounts for the observed experimental value.

3.3. Deamination of a Tautomer of Cytosine with $2H_2O$: Pathway F. We also considered the possibility of the $Cyt^-\cdots H_2O\cdots H_2O$ complex being protonated. Computational studies also have predicted that cytosine protonation in aqueous solution or in the gas phase should occur at the N_3 position[25–29] (see Figure 1). Protonation occurred at the N_3 site, known to be more favorable site for protonation of cytosine,[29] resulting in a complex of the amino-oxo tautomer of cytosine with two water molecules. This resulted in a new pathway designated as pathway F. The geometries for the reactant, intermediates, transition state, and product are show in Figure 11, while the relative energies are shown in Figure 12. Activation energies, enthalpies of activation, and free energies of activation for pathway F at MP2 and B3LYP levels of theory using the 6-31G(d) basis set, B3LYP/6-31+G(d), and G3MP2 levels of theory are listed in Table 5.

Pathway F is a mechanism with a single rate-determining step and several conformational changes connecting intermediates $I1_F$ and $I2_F$. The first and last steps are similar to the previous pathways. Interestingly, the barriers for $TS1_F$ and $TS2_F$ increase for pathway F compared to TS1 and $TS2_C$ for pathway C from 115.3 to 140.9 kJ mol^{-1} and from 68.3 to 92.6 kJ mol^{-1} at G3MP2 level of theory, respectively. The first step is the rate-determining step with a barrier of 140.9 and 129.6 kJ mol^{-1} at G3MP2 and B3LYP/6-31+G(d) levels of theory, respectively, which is high compared to the experimental value.

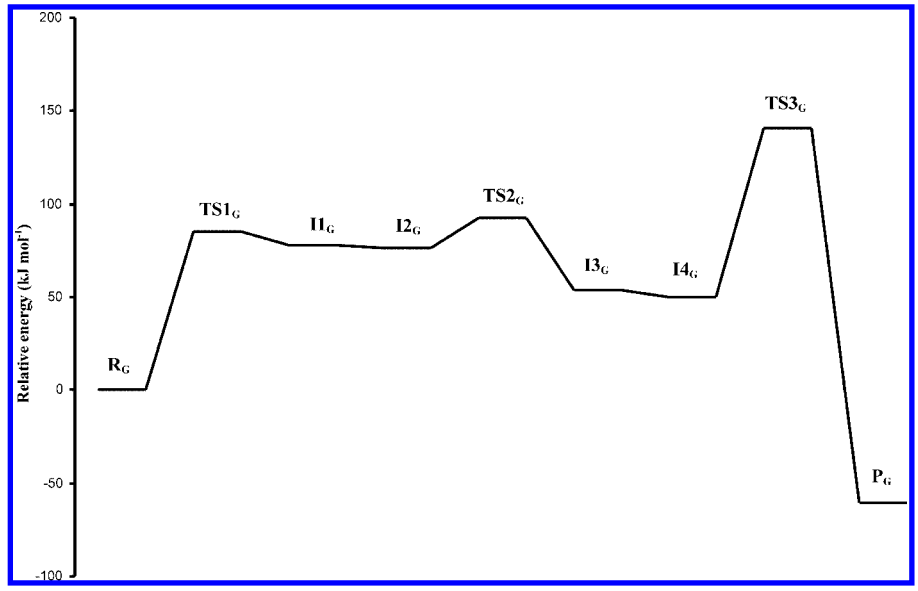

Figure 15. Reaction pathway G for the deamination of cytosine with $2H_2O/OH^-$. Relative energies are at the G3MP2 level of theory.

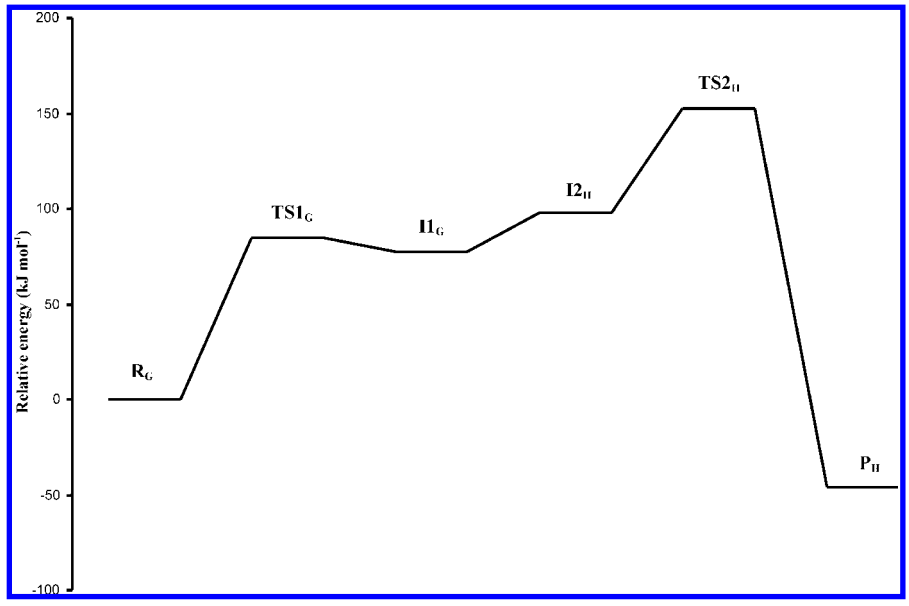

Figure 16. Reaction pathway H for the deamination of cytosine with $2H_2O/OH^-$. Relative energies are at the G3MP2 level of theory.

Table 6. Activation Energies, Enthalpies of Activation, and Free Energies of Activation for the Deamination of Cytosine with $2H_2O/OH^-$ (in kJ mol^{-1}) at 298.15 K (Pathway G)

	MP2/ 6-31G(d)	B3LYP/ 6-31G(d)	B3LYP/ 6-31+G(d)	G3MP2
ΔE_{act}, $TS1_G$	76.1	96.6	110.9	84.8 (86.5)[a]
$\Delta H^{\ddagger}$, $TS1_G$	79.3	99.8	112.3	82.0
$\Delta G^{\ddagger}$, $TS1_G$	91.1	112.6	123.9	93.5
ΔE_{act}, $TS2_G$	22.8	16.4	16.7	16.2 (18.9)
$\Delta H^{\ddagger}$, $TS2_G$	9.9	4.2	4.7	12.4
$\Delta G^{\ddagger}$, $TS2_G$	17.4	10.6	12.5	23.4
ΔE_{act}, $TS3_G$	106.1	83.0	75.5	90.3 (94.5)
$\Delta H^{\ddagger}$, $TS3_G$	86.7	63.8	61.4	90.2
$\Delta G^{\ddagger}$, $TS3_G$	83.6	58.1	54.8	89.5

[a] The values in bracket are for MP2/G3MP2Large.

Table 7. Activation Energies, Enthalpies of Activation, and Free Energies of Activation for the Deamination of Cytosine with $2H_2O/OH^-$ (in kJ mol^{-1}) at 298.15 K (Pathway H)

	MP2/ 6-31G(d)	B3LYP/ 6-31G(d)	B3LYP/ 6-31+G(d)	G3MP2
ΔE_{act}, $TS1_G$	76.1	96.6	110.9	84.8 (86.5)[a]
$\Delta H^{\ddagger}$, $TS1_G$	79.3	99.8	112.3	82.0
$\Delta G^{\ddagger}$, $TS1_G$	91.1	112.6	123.9	93.5
ΔE_{act}, $TS2_H$	57.1	35.2	57.6	55.3 (50.6)
$\Delta H^{\ddagger}$, $TS2_H$	41.3	21.4	46.9	51.5
$\Delta G^{\ddagger}$, $TS2_H$	53.8	30.5	55.9	63.6

[a] The values in bracket are for MP2/G3MP2Large.

3.4. Deamination of Cytosine with $2H_2O/OH^-$: Pathways G and H. Since the presence of a single water molecule had a significant effect on the various reaction pathways, we have investigated the effect of a second water molecule on the potential energy surface for pathways C and D. The geometries of the reactants, intermediates, transition states, and products for pathways G and H are shown in Figures 13 and 14, respectively. The relative energies for pathways G and H are shown in Figures 15 and 16, respectively. The activation energies, enthalpies of activation, and free energies of activation for pathways G and H are listed in Tables 6 and 7, respectively.

The key steps for pathways G and H are similar to the previous pathways C and D. Addition of the second water molecule further reduces the barriers for both rate-determining steps. For pathway G, the product (P_G) is a complex of the uracil anion, two water molecules, and ammonia ($Ura^- \cdots 2H_2O \cdots NH_3$) at the MP2/6-31G(d), B3LYP/6-31G(d), and B3LYP/6-31+G(d) levels of theory with a negative charge at the N_1 atom, which is not possible in DNA and RNA (cytosine is chemically bound to the sugar moiety at N_1 in DNA).

For pathways G and H, we note that adding the second water molecule reduces the activation energy of the first-step (which is the same for both pathways) by 30.5 kJ mol^{-1} at G3MP2 and by a lesser amount for the other steps. This is due to the fact that the second water molecule can both stabilize the transition state and act as a catalyst for this system. The activation energies for the two rate-determining steps are 84.8 and 90.3 kJ mol^{-1} for pathway G and 84.8 and 55.3 kJ mol^{-1} for pathway H at G3MP2 level of theory. However, the overall activation energies for pathways G and H are 140.5 and 152.9 kJ mol^{-1} at G3MP2 (134.6 and 155.6 kJ mol^{-1} at B3LYP/6-31+G(d)), respectively, see Tables 6 and 7, which are still high compared to the experimental value. For pathway G intermediate $I3_G$, similarly to intermediate $I3_D$, would most likely be protonated at the $-NH_2$ group. The first step would then be the rate-determining step with an activation energy of only 93 kJ mol^{-1} at G3MP2. This lower barrier may account for the difference between the deamination of free cytosine versus cytosine in single-stranded DNA.

4. CONCLUSIONS

The mechanism for the deamination reaction of cytosine with H_2O/OH^- and $2H_2O/OH^-$ to produce uracil was investigated using ab initio calculations. Seven pathways for the deamination reaction were found. This paper shows the first detailed study of possible mechanisms for the deamination reaction of cytosine with OH^- including the effect of the presence of one and two water molecules. In all the mechanisms, a series of conformational changes connect the transition states of the two rate-determining steps. Pathway D is the first plausible mechanism reported for the deamination of cytosine, where the calculated activation energy (115.3 kJ mol^{-1} at G3MP2 level of theory) agrees very well with the experimentally determined activation energy (117 $\pm$ 4 kJ mol^{-1}).

ACKNOWLEDGMENT

We thank the Natural Sciences and Engineering Council of Canada (NSERC) for financial support. We gratefully acknowledge the Atlantic Computational Excellence Network (ACEnet) for computer time.

Supporting Information Available: Full geometries and energies of all structures for all pathways investigated at all levels of theory used. This information is available free of charge via the Internet at http://pubs.acs.org.

REFERENCES AND NOTES

(1) Saenger, W. *Principles of Nucleic Acid Structure*; Springer-Verlag: New York, 1984.

(2) Neidle, S. *Oxford Hand Book of Nucleic Acid Structure*; Oxford University Press Inc.: New York, 1999.

(3) Almatarneh, M. H.; Flinn, C. G.; Poirier, R. A.; Sokalski, W. A. Computational Study of the Deamination Reaction of Cytosine with H_2O and OH^-. *J. Phys. Chem. A* **2006**, *110*, 8227–8234.

(4) Peng, W.; Shaw, B. R. Accelerated Deamination of Cytosine Residues in UV-Induced Cyclobutane Pyrimidine Dimers Leads to CC → TT Transitions. *Biochemistry* **1996**, *35*, 10172–10181.

(5) Notari, R. E.; Chin, M. L.; Cardoni, A. Intermolecular and Intramolecular Catalysis in Deamination of Cytosine Nucleosides. *J. Pharm. Sci.* **1970**, *59*, 28–32.

(6) Yao, L.; li, Y.; Wu, Y.; Liu, A.; Yan, H. Product Release Is Rate-Limiting in the Activation of the Prodrug 5-Fluorocytosine by Yeast Cytosine Deaminase. *Biochemistry* **2005**, *44*, 5940–5947.

(7) Shapiro, R.; Servis, R. E.; Wecher, M. Reactions of Uracil and Cytosine Derivatives with Sodium Bisulfite. *J. Am. Chem. Soc.* **1970**, *92*, 422–424.

(8) Shapiro, R.; Klein, R. Reactions of Cytosine Derivatives with Acidic Buffer Solutions. II. Studies on Transamination, Deamination, and Deuterium Exchange. *Biochemistry* **1967**, *6*, 3576–3582.

(9) Merchant, K.; Chen, H.; Gonzalez, T. C.; Keefer, L. K.; Shaw, B. R. Deamination of Single-Stranded DNA Cytosine Residues in Aerobic Nitric Oxide Solution at Micromolar Total NO Exposures. *Chem. Res. Toxicol.* **1996**, *9*, 891–896.

(10) Dreyfus, M.; Bensaude, O.; Dodin, G.; Dubois, J. E. Tautomerism in Cytosine and 3-Methylcytosine. A Thermodynamic and Kinetic Study. *J. Am. Chem. Soc.* **1976**, *98*, 6338–6349.

(11) Shapiro, R.; Klein, R. The Deamination of Cytidine and Cytosine by Acidic Buffer Solutions. Mutagenic Implications. *Biochemistry* **1966**, *5*, 2358–2362.

(12) Chen, H.; Shaw, B. R. Bisulfite Induces Tandem Double CC → TT Mutations in Double-Stranded DNA. 2. Kinetics of Cytosine Deamination. *Biochemistry* **1994**, *33*, 4121–4129.

(13) Bobek, M.; Cheng, Y. C.; Bloch, A. Novel Arabinofuranosyl Derivatives of Cytosine Resistant to Enzymic Deamination and Possessing Potent Antitumor Activity. *J. Med. Chem.* **1978**, *21*, 597–598.

(14) Duncan, B. K.; Miller, J. H. Mutagenic Deamination of Cytosine Residues in DNA. *Nature* **1980**, *287*, 560–561.

(15) Frederico, L. A.; Kunkel, T. A.; Shaw, B. R. A Sensitive Genetic Assay for the Detection of Cytosine Deamination: Determination of Rate Constants and the Activation Energy. *Biochemistry* **1990**, *29*, 2532–2537.

(16) Lindahl, T.; Nyberg, B. Heat-Induced Deamination of Cytosine Residues in Deoxyribonucleic Acid. *Biochemistry* **1974**, *13*, 3405–3410.

(17) Sponer, J. E.; Miguel, P. J.; Rodriguez-Santiago, L.; Erxleben, A.; Krumm, M.; Sodupe, M.; Sponer, J.; lippert, B. Metal-Mediated Deamination of Cytosine: Experiment and DFT Calculations. *Angew. Chem., Int. Ed.* **2004**, *43*, 5396–5399.

(18) Rayat, S.; Qian, M.; Glaser, R. Nitrosative Cytosine Deamination. An Exploration of the Chemistry Emanating from Deamination with Pyrimidine Ring-Opening. *Chem. Res. Toxicol.* **2005**, *18*, 1211–1218.

(19) Matsubara, T.; Ishikura, M.; Aida, M. A Quantum Chemical Study of the Catalysis for Cytidine Deaminase: Contribution of the Extra Water Molecule. *J. Chem. Inf. Model.* **2006**, *46*, 1276–1285.

(20) Flinn, C.; Poirier, R. A.; Sokalski, W. A. Ab Initio Study of the Deamination of Formamidine. *J. Phys. Chem. A* **2003**, *107*, 11174–11181.

(21) Fogarasi, G.; Szalay, P. G. The interaction Between Cytosine Tautomers and Water: an MP2 and Coupled Cluster Electron Correlation Study. *Chem. Phys. Lett.* **2002**, *356*, 383–390.

(22) Frisch, M. J.; Trucks, G. W.; Schlegel, H. B.; Scuseria, G. E.; Robb, M. A.; Cheeseman, J. R.; Montgomery, J. A., Jr.; Vreven, T.; Kudin, K. N.; Burant, J. C.; Millam, J. M.; Iyengar, S. S.; Tomasi, J.; Barone, V.; Mennucci, B.; Cossi, M.; Scalmani, G.; Rega, N.; Petersson, G. A.; Nakatsuji, H.; Hada, M.; Ehara, M.; Toyota, K.; Fukuda, R.; Hasegawa, J.; Ishida, M.; Nakajima, T.; Honda, Y.; Kitao, O.; Nakai, H.; Klene, M.; Li, X.; Knox, J. E.; Hratchian, H. P.; Cross, J. B.; Bakken, V.; Adamo, C.; Jaramillo, J.; Gomperts, R.; Stratmann, R. E.; Yazyev, O.; Austin, A. J.; Cammi, R.; Pomelli, C.; Ochterski, J. W.; Ayala, P. Y.; Morokuma, K.; Voth, G. A.; Salvador, P.; Dannenberg, J. J.; Zakrzewski, V. G.; Dapprich, S.; Daniels, A. D.; Strain, M. C.; Farkas, O.; Malick, D. K.; Rabuck, A. D.; Raghavachari, K.; Foresman, J. B.; Ortiz, J. V.; Cui, Q.; Baboul, A. G.; Clifford, S.; Cioslowski, J.; Stefanov, B. B.; Liu, G.; Liashenko, A.; Piskorz, P.; Komaromi, I.; Martin, R. L.; Fox, D. J.; Keith, T.; Al-Laham, M. A.; Peng, C. Y.; Nanayakkara, A.; Challacombe, M.; Gill, P. M. W.; Johnson, B.; Chen, W.; Wong, M. W.; Gonzalez, C.; Pople, J. A. *Gaussian 03*, revision B.05; Gaussian, Inc.: Wallingford, CT, 2004.

(23) Almatarneh, M. H.; Flinn, C. G.; Poirier, R. A. Ab initio Study of the Decomposition of Formamidine. *Can. J. Chem.* **2005**, *83*, 2082–2090.

(24) Snider, M. J.; Reinhardt, L.; Wolfenden, R.; Cleland, W. W. ^{15}N Kinetic Isotope Effects on Uncatalyzed and Enzymatic Deamination of Cytidine. *Biochemistry* **2002**, *41*, 415–421.
(25) Floriøn, J.; Baumruk, V.; Leszczyński, J. IR and Raman Spectra, Tautomeric Stabilities, and Scaled Quantum Mechanical Force Fields of Protonated Cytosine. *J. Phys. Chem.* **1996**, *100*, 5578–5589.
(26) Hunter, K. C.; Wetmore, S. D. Hydrogen-Bonding Between Cytosine and Water: Computational Evidence for a Ring-Opened Complex. *Chem. Phys. Lett.* **2006**, *422*, 500–506.
(27) Hunter, K. C.; Rutledge, L. R.; Wetmore, S. D. The Hydrogen Bonding Properties of Cytosine: A Computational Study of Cytosine Complexed with Hydrogen Fluoride, Water, and Ammonia. *J. Phys. Chem. A* **2005**, *109*, 9554–9562.
(28) Tureček, F.; Yao, C. Hydrogen Atom Addition to Cytosine, 1-Methylcytosine, and Cytosine-Water Complexes. A Computational Study of a Mechanistic Dichotomy. *J. Phys. Chem. A* **2003**, *107*, 9221–9231.
(29) Zhang, H.; Liang, Q.; Xia, Y.; Zhao, M.; Ji, Y.; Song, C.; Liu, X.; Zhang, B. Theoretical Study of the ·H Reaction with Cytosine. *Int. J. Quantum Chem.* **2007**, *107*, 240–246.

CI7003219